SCIENCE OBSERVATION STRATEGY FOR HAYABUSA-2 OPTICAL NAVIGATION CAMERAS (ONC). S. Sugita[1], T. Morota[2], S. Kameda[3], R. Honda[4], C. Honda[5], and Hayabusa-2 ONC Science Team, [1]Univ. of Tokyo, Kashiwa, Chiba, JAPAN (sugita@k.u-tokyo.ac.jp), [2]Nagoya Univ. [3]Rikkyo Univ., [4]Kochi Univ., [5]Aizu Univ.

Instrument Overview: Optical Navigator Cameras (ONC) will be used for scientific imaging observations as well as for the Hayabusa-2 spacecraft navigation in the proximity of asteroid 1999 JU_3. The ONC system consists of the three subsystems, a telescopic camera (ONC-T) and wide-angle cameras (ONC-W1 and -W2). Each subsystem has a two-dimensional (1024×1024) charge-coupled device (CCD) sensitive to wavelengths between 350 and 1060 nm. Both ONC-T and W1 are installed on the bottom of spacecraft (i.e., –Z panel) for nadir view, and ONC-W2 is on the side of spacecraft (–X panel) for slant view (Fig. 1). The effective field of view (FOV) of ONC-T is 5.7 × 5.7 deg, and that of ONC-W1 and W2 are 60 × 60 deg. The spatial resolution at 1 km altitude is 0.1 m/pixel for ONC-T and 1.0 m/pixel for ONC-W1 and W2, respectively. ONC-T has a broad band-pass filter (0.35 – 1.2 μm), six medium-breadth filters ($0.39_{\pm 20}$, $0.48_{\pm 15}$, $0.55_{\pm 15}$, $0.70_{\pm 15}$, $0.86_{\pm 20}$, and $0.95_{\pm 30}$; suffixes indicate the respective band widths)), and a narrow band Na filter at 0.59 μm with 10 nm of FWHM.

Basic Operations Phases: The scientific observations of ONC are planned to be conducted in the following five different phases depending on the distances to the asteroid. (1) Cruising phase is between the deployment of Hayabusa 2 to its orbit to 1999 JU_3 and arrival at the home position (HP) 20 km from the asteroid. Bright stars, Earth, and perhaps Moon will be observed for camera calibrations during this phase. Measurements of the light curves and disk-averaged spectra of 1999 JU_3 will also be conducted as well as search for a satellite of 1999JU_3. (2) During the HP phase, both single-band (0.55μm) observations for shape modeling and six-band observations for spectroscopic characterization will be conducted globally with 2 m/pixel resolution. (3) Low-altitude-phase observations will be conducted at 5, 1, and/or 0.1 km of altitudes for local areas for detailed mapping in order to characterize sampling site candidates and to look for a SCI-generated impact crater. (4) Lander-deployment-phase observations will be conducted with W2 immediately after lander deployment, with W1 during the subsequent ascent of Hayabusa-2, and with ONC-T at 1 km altitude for locating both MASCOT and MINERVA's. (5) Touchdown-phase observations will be conducted before, during, and after each sampling touchdown (TD). Although ONC will be used exclusively for navigations at altitudes between 50 to 5 m during TD descent, science observations will be conducted at the other altitudes during descent ant all the altitudes during ascent.

Morphological Observations: The shape and surface morphology of 1999 JU_3 will be observed with the 0.55 μm filter globally from HP and locally from lower altitudes with much higher resolutions. The morphology of 1999JU_3 provides information about its geologic history and large-scale structure, such as whether it is a rubble pile or monolithic. Such information is indispensable for understanding the formation mechanism, the source region, and the parent body of 1999 JU_3. The global shape model of 1999 JU_3 will be reconstructed with the HP global mapping images with various shape reconstruction techniques (e.g., limb profiles, stereogrammetric procedure, shape from shading, and/or photometric stereo). Global shape reconstruction allows us to estimate the asteroid volume, which is necessary for bulk density estimate. Bulk density is important for distinguishing a rubble pile and a monolith. We are planning to estimate the volume with accuracy of ~5% to have ~7% of bulk density accuracy.

The morphology and size distribution of craters and boulders on 1999 JU_3 are necessary for understanding the collisional history of 1999 JU_3. For example, the crater size-frequency measurement on 1999 JU_3 will help us estimate the formation age of 1999 JU_3 or the timing of the latest resurfacing event occurred on 1999 JU_3. The size and shape distributions of the boulders will also help us finding out whether these boulders are original fragments from the disruption of the larger parent body of 1999 JU_3 or are fragments from more recent impact cratering on 1999 JU_3. For these purposes, we should identify craters and boulders larger than 20 m in diameter with the global mapping data and larger than 1 m in diameter with close-up images obtained from 1 km altitude, respectively.

The SCI experiment provides critical "ground-truth" information about the relationship between impact energy and crater size on asteroid, which has not been well understood. The SCI crater size depends heavily on the physical properties and surface structure of 1999 JU_3. Based on the scaling laws derived from numerical simulations and laboratory experiments of impact cratering, the SCI crater diameter is estimated to be 1-10 m for fine-particle targets, or a few tens of cm for high-porosity targets or rock targets. Therefore the spatial resolution of close-up images required for searching the SCI crater should be better than 10 cm/pixel.

Multi-band spectroscopy with ONC-T: The six medium-breadth filters will be used for multiband spectroscopic observations. These observations allow us to characterize the overall spectroscopic properties of different parts of the asteroid surface. There have been a variety of different visible spectra observed for asteroid 1999 JU_3 [e.g., 1-6]. Although there may be actually no real spectral variation on 1999 JU_3 surface, there may be a great spectral variegation as well [6]. Thus, it is very important to quantify the degree of such possible inhomogeneity accurately before conducting detailed observations. Previous observations and analyses of the spectra of both main-belt and near-earth asteroids indicate that they can be divided into well-defined types based on a small number of principal components [7]. A similar approach will be useful for describing the overall spectroscopic properties of each part of 1999 JU_3 surface, allowing us to compare it with the spectra of asteroids and meteorites quantitatively. Although principal component analysis results do not necessarily give us direct information on material properties of asteroids, it is very useful for quantifying the degree of inhomogeneity, finding spectroscopic trends, and distinguishing different geologic units.

From these spectroscopic data, a variety of material properties can also be estimated. For example, a broad absorption band around 0.7 μm has been found for many main belt asteroids and has been interpreted to be due to serpentine [8]. Such absorption will be detected with three filters at 0.55, 0.70, and 0.86 μm. Also, the degree of absorption in the UV range, which is another index for hydrous minerals, will be quantified with images with 0.39, 0.48, and 0.55 μm filters. Heating experiments, an analogue for dehydration processes, such as space weathering, indicates that this short wavelength range reflectance of carbonaceous chondrites changes rather sensitively as a function of heating temperature [9]. Furthermore, the distribution of albedo on the surface will be mapped globally, which is a byproduct of high-resolution shape model of the asteroid. The surface albedo (e.g., at 0.55 μm) will serve as a good index for insoluble organic matter (IOM), which comprises of the majority of carbon content of carbonaceous meteorites [10].

These observations will help us estimating the distribution of hydrous minerals, organics, and space weathering. Such information will be key for both understanding of the history of this asteroid and sampling site selection.

Exospheric Na: Emission from exospheric Na around 1999 JU_3 is detectable by ONC-T with the 0.59 μm filter if the Na source rate on 1999 JU_3 is comparable with that on Moon. Because Na is one of the most volatile metallic elements, it would be lost upon heating; Na depletion would occur at ~ 630°C [e.g., 11]. This Na depletion temperature is much higher than disappearance temperatures 400°C for 0.7μm and comparable to 600°C for 3 μm absorption bands, respectively [9]. Moreover, the exospheric Na of planetary bodies is supplied from centimeters depth of subsurface, while the reflectance spectroscopy of solid surfaces is controlled by only a sub-millimeter thick surface layer. Thus, if the cm's-deep subsurface on1999 JU_3 has not been heated at temperatures > 630°C, its Na abundance is probably higher than Mercury and Moon. Then, a tenuous but detectable Na atmosphere could be formed around the asteroid. If the heating history of 1999 JU_3 surface is not uniform, exospheric Na distribution would exhibit non-uniformity. Such observations will be useful for understanding the devolatilization state of 1999 JU_3 and helpful for selecting the touchdown site. This information will be extremely useful if clear signature of hydrous minerals, such as 0.7μm or 3μm absorption bands, is not observed on 1999 JU_3 surface from HP.

References: [1] Binzel, R. P. *et al*., 2001, *Icarus*, *151*, 139-149. [2] Vilas, F., 2008, *Astron. J.*, *135*, 1101-1105. [3] Sugita, S. *et al.*, 2012, *DPS Mtg. 44*, #102.02. [4] Moskovitz, N. et al., 2012, *DPS Mtg. 44*, #102.04. [5] Lazzaro, D. *et al.*, 2013, *Astron. Astrophys.*, in press. [6] Sugita, S. *LPSC*, *44*, #2591, [7] Bus, S. and Binzel, R. P., 2002, *Icarus*, *158*, 146-177. [8] Vilas & Gaffey, 1989, *Science*, *246*, 790. [9] Hiroi, T. et al., 1996, *MAPS*, *31*, 321-327. [10] Cronin et al., 1988, in *Meteorites and the Early Solar System*, pp. 819–860. [11] Kasuga, T. *et al*., 2006, *Astron. Astrophys.*, *453*, L17-20.

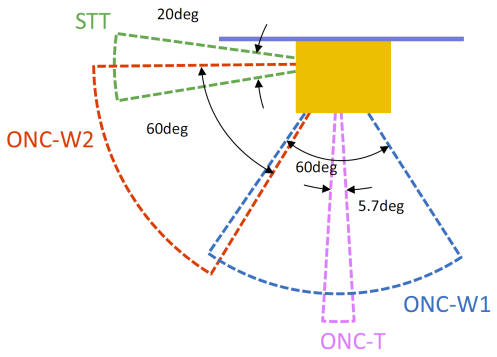

Figure 1. Comparison of field of view for the three ONC subsystems (T, W1, and W2) and the star tracker (STT). The blue line in the illustration is the solar panel array on the top of the spacecraft body.